

3. (a) S. Nishikiori and T. Iwamoto, *Chem. Lett.*, 319 (1984); (b) S. Nishikiori and T. Iwamoto, *Chem. Lett.*, 1129 (1983); (c) T. Hasegawa, S. Nishikiori, and T. Iwamoto, *Chem. Lett.*, 1659 (1985). (d) S. Nishikiori and T. Iwamoto, *Chem. Lett.*, 1127 (1987).
4. M. Fujita, J. Yazaki, and K. Ogura, *J. Am. Chem. Soc.*, **112**, 5645 (1990).
5. (a) D. Evans, J. A. Osborn and G. Wilkinson, *Inorg. Syn.*, **11**, 99 (1968); (b) K. Vrieze, J. P. Collman, C. T. Sears, and M. Kubota, *Inorg. Syn.*, **11**, 101 (1968).
6. D. J. Liston, Y. J. Jee, W. R. Scheidt, and C. A. Reed, *J. Am. Chem. Soc.*, **111**, 6643 (1989).
7. J. H. Bigelow, *Inorg. Syn.*, **2**, 250 (1946).
8. W. R. Mason and H. B. Gray, *J. Am. Chem. Soc.*, **90**, 5721 (1968).
9. G. K. N. Reddy and B. R. Ramesh, *J. Organomet. Chem.*, **87**, 347 (1975).
10. G. K. N. Reddy and B. R. Ramesh, *Indian J. Chem. Chem. Sect. A.*, **15A**, 621 (1977).
11. J. Peone, Jr. and L. Vaska, *Angew. Chem. Int. Ed. Engl.*, **10**, 511 (1971).
12. (a) J. L. Burmeister and N. J. DeStefano, *Inorg. Chem.*, **8**, 1546 (1969); (b) D. M. L. Goodgame and M. A. Hitchman, *Inorg. Chem.*, **3**, 1389 (1964).
13. D. A. MacInnes, "The Principles of Electrochemistry", Dover, New York, p. 342 (1961).
14. J. S. Krieff and D. F. Shriver, *Inorg. Chem.*, **12**, 1788 (1975).
15. L. E. Manzer and G. W. Parshall, *Inorg. Chem.*, **15**, 3114 (1976).
16. H. M. Jeong and C. S. Chin, *Bull. Kor. Chem. Soc.*, **7**, 468 (1986).
17. J. A. Abys, G. Ogar, and W. M. Risen, Jr., *Inorg. Chem.*, **20**, 4446 (1981).

## Photodissociation of CINO at 236 nm

Hong Lae Kim\*, Yuxiang Mo<sup>†</sup>, Yutaka Matsumi<sup>‡</sup>, and Masahiro Kawasaki<sup>‡</sup>

*Department of Chemistry, Kangweon National University, Chuncheon 200-701*

*<sup>‡</sup>Research Institute of Applied Electricity, Hokkaido University, Sapporo 060, Japan*

*Received November 13, 1991*

The fine structure branching ratio and Doppler profiles of photofragment Cl (<sup>2</sup>P<sub>1/2</sub>) atoms from photodissociation of CINO around 236 nm in the A band have been measured by the two photon resonance enhanced multiphoton ionization technique. The measured branching ratio, Cl\* (<sup>2</sup>P<sub>1/2</sub>)/Cl (<sup>2</sup>P<sub>3/2</sub>) is 0.18 ± 0.02. The Doppler profile of Cl is well reproduced assuming that one of the two components in the photofragment translational spectra reported by Haas, Felder, and Huber [*Chem. Phys. Lett.*, **180**, 293 (1990)] should correspond to Cl and that an anisotropy parameter β for the angular distribution is 0.45. The results suggest that CINO dissociation in the A band should consist of at least two non-crossing electronic states which correlate to the formation of Cl\* and Cl, respectively.

### Introduction

Photodissociation of small polyatomic molecules has been the subject of great interest because the system is simple enough to be studied theoretically and experimentally. Extensive theories such as the Frank-Condon theory or the sudden approximation in quantum scattering theory have been developed to explain the dynamics of the dissociation.<sup>1</sup> CINO is a typical bent triatomic molecule appropriate for theoretical calculations. In addition, spectroscopy of CINO and of the fragments Cl and NO has been well studied experimentally. Thus, the study of photodissociation dynamics of CINO has been focused on for many years since the pioneering work by Busch and Wilson.<sup>2</sup> Since the shape of potential energy surfaces in upper states determines the dynamics of the dissociation, electronic structure calculations can help understanding the dynamics of the process. Once the potential energy surfaces are known, the theory can predict

the detailed dynamics of the process such as mechanism and distributions of available energies among various degrees of freedom of the products. On the other hand, certain experimental observables which can explain the dynamics such as the energy and the angular distributions of the products deduce the approximate shape of the potential energy surfaces. Therefore, it is of fundamental importance to measure the energy and the angular distributions of the products in order to map out the potential surfaces in the excited state.

CINO shows several absorptions in the UV-VIS region which are called the A, B, C, D, and E bands (Figure 1).<sup>3</sup> Recent *ab initio* calculations and experimental studies of photodissociation following the excitation of these bands can assign them as (1) E band-T<sub>1</sub>←S<sub>0</sub>, (2) D and C band-S<sub>1</sub>←S<sub>0</sub>, (3) B band-S<sub>3</sub>←S<sub>0</sub>, (4) A band-S<sub>5</sub>←S<sub>0</sub>, respectively.<sup>3-6</sup> Extensive studies have been carried out for the dissociation from the E, C, and B bands by detecting LIF from the NO products. This LIF technique has high enough sensitivity to determine the rotational energy distributions of NO with the resolution of the λ doublet. In addition, vector properties

<sup>†</sup>On leave from Dalian Institute of Chemical Physics, Chinese Academy of Science, Dalian, China.

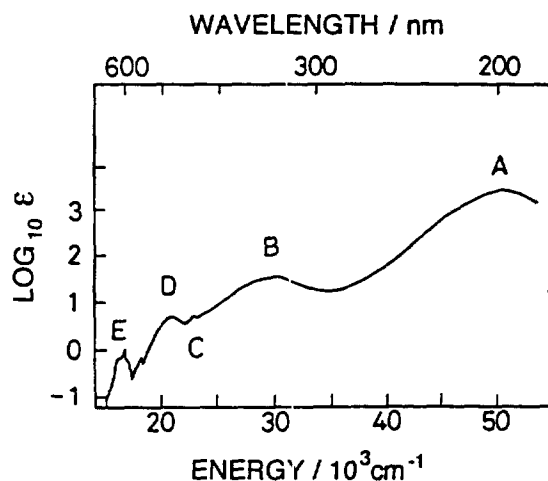


**Figure 1.** The absorption spectrum of ClNO in the UV-VIS region cited from ref. 3.

of the products have been determined to reveal the symmetries of the excited states and stereochemistry of the dissociation. On the other hand, Bell *et al.* reported resonance enhanced Raman spectra of ClNO at 514, 420, and 355 nm, which correspond to electronic excitations to the D, C and B bands, respectively.<sup>7</sup> No overtones were observed at any wavelengths they investigated. From the results, they concluded that the dissociation of ClNO may not be as fast as was previously thought.

Photodissociation of ClNO following the excitation of the A band has been carried out at 248 and 193 nm.<sup>8</sup> The vibrational energy distribution of NO has been measured by infrared fluorescence. The measured vibrational distribution is highly inverted and about 40% of the available energy goes into translation. Most recently, Huber and coworkers measured the translational energies and angular distribution of the products using photofragment translational spectroscopy.<sup>9</sup> They found two different translational energy distributions in the products resulting from the two different vibrational energy distributions of the NO fragments. Based on the different angular distributions of the products that were also observed, they concluded two dissociative channels arising from the two different ClNO excited states. The one channel produces Cl and the other produces Cl\* in the other spin-orbit state.

In this study, we firstly report the spectra of Cl and Cl\* produced from the photodissociation of ClNO around 236 nm using REMPI. The spectra confirm the two different excited states in the A band leading to dissociation according to the correlation diagram. In addition, the branching ratio Cl\*/Cl can tell us the symmetries of the excited states and the adiabaticity of the dissociation. We measured the translational energy and deduced the anisotropy parameter by analyzing the Doppler profiles of the spectra.

## Experiment

The experimental apparatus was described in detail in the previous report.<sup>10</sup> Briefly, ClNO was introduced into a vacuum chamber through a pulsed nozzle in the form of an effusive beam. The molecular beam crossed the laser beam

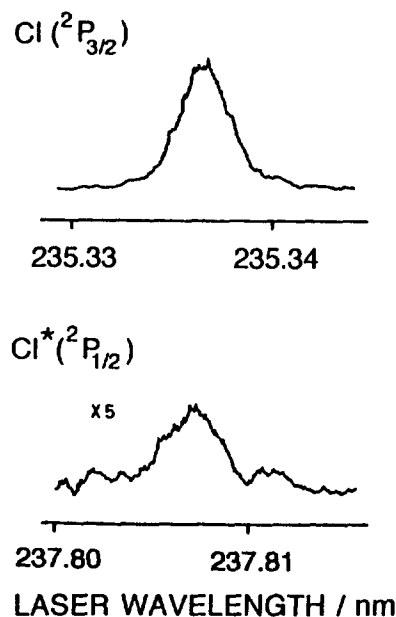


**Figure 2.** REMPI spectra of Cl and Cl\* produced from photodissociation of ClNO.

at a right angle. A dye laser output (Lambda Physik FL3002 E) pumped by a XeCl excimer laser (Questek 2520) was doubled with a BBO crystal. The UV light dissociated the sample and ionized the Cl and Cl\* products with successive photons. The background pressure of the chamber was about  $2 \times 10^{-6}$  torr while the pressure was  $1 \times 10^{-5}$  torr with the sample running.

The spectra of Cl were measured by a (2+1) REMPI method. Cl has two different spin-orbit states with the total angular momentum  $j=1/2$  and  $2/3$ . The energy of Cl in the  $^2P_{3/2}$  state is lower than Cl in  $^2P_{1/2}$  by  $880 \text{ cm}^{-1}$ . The two photon absorption at  $235.3 \text{ nm}$  for  $4p \ ^2D_{3/2} \leftarrow 3p \ ^2P_{3/2}$  or at  $237.8 \text{ nm}$  for  $4p \ ^2D_{3/2} \leftarrow 3p \ ^2P_{1/2}$  is the bottleneck of this REMPI process. The relative absorption cross section was previously measured to be unity.<sup>11</sup> The bandwidth of the dye laser was  $0.2 \text{ cm}^{-1}$ . When an intracavity etalon was installed, the resolution of the spectra was  $0.1 \text{ cm}^{-1}$  for Doppler profile measurements. Ions were collected by an ion optical system where an electron multiplier was employed. The output of the electron multiplier was amplified, fed into a Boxcar averager, and stored in a PC for further processing. The detection chamber separated with a slit of a meshed screen from the main chamber was pumped separately. A care was always taken to avoid saturation in the spectra.

ClNO was prepared by mixing  $\text{Cl}_2$  and NO (1 : 1.5 mixture) and used without further purification.

## Results

Photodissociation of ClNO had to be done at two different wavelengths, that is 235.3 and 237.8 nm where the two photon transitions of Cl and Cl\* showed their maxima, respectively, because a single laser had been used for both photodissociation and probe. Fortunately, the absorption spectrum of the A band shows a broad band around these wavelengths. Thus, we assume the absorption cross section to be not much

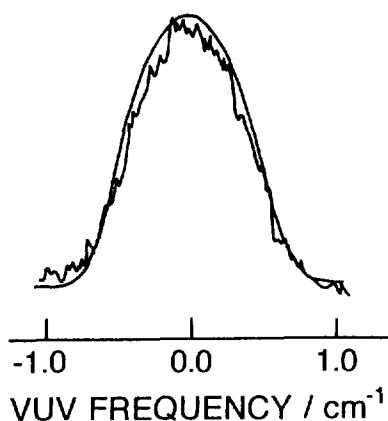


**Figure 3.** The spectrum of Cl under high resolution. The smooth curve is the simulated Doppler profile (see text).

different at these two wavelengths as well as the branching ratio.

The measured spectra of Cl and Cl\* are displayed in Figure 2. The branching ratio of Cl\*/Cl was calculated from the areas under the two curves after the correction of the probe laser power. We measured the spectra as a function of the probe laser power. The slope of the straight line appeared to be 2.35 when we plotted the calibrated MPI signal in terms of the laser power, which was typical in the one-color experiment. The measured branching ratio is  $0.18 \pm 0.02$ .

In Figure 3, the spectrum of Cl is shown under high resolution for the Doppler profile analysis. The Doppler profile is given by<sup>12</sup>

$$g(\chi_D) = [1 + \beta P_2(\cos \alpha) P_2(\chi_D)] (2\Delta\nu_0)^{-1}$$

where  $g(\chi_D)$  is the line shape function,  $\chi_D$ , the Doppler shift equal to  $(v \cdot k/c)v_0$ ,  $v$ , the velocity of the fragment,  $k$ , the propagation direction of the probe light,  $\alpha$ , the angle between the polarization direction of the dissociating laser light and  $k$ , (in our case  $\alpha = \pi/2$ ),  $\Delta\nu_0$ , the maximum frequency shift from the line center,  $\beta$ , the recoil anisotropy parameter, and  $P_2$ , the second order Legendre function,  $P_2(x) = (3x^2 - 1)/2$ . We simulated the observed profile with a suitable  $\beta$  value and the reported translational energy distribution for Cl obtained by Haas *et al.*<sup>9</sup> Assuming the anisotropy parameter ( $\beta = 0.45$ ) and the broader energy distribution of Haas *et al.*, our Doppler profile is well reproduced with the average translational energy of 34 kcal/mol. Since the available energy at 235.3 nm from the dissociation is 84 kcal/mol, the fraction of the translational energy is about 0.4. This is in good agreement with the previous experiments done in the A band.<sup>8,9</sup>

## Discussions

Photodissociation of ClNO in the A band around 236 nm has been investigated by measuring the spectra of Cl and Cl\* using REMPI. The fraction of the translational energy measured from the Doppler profiles is 0.4 which is similar to the values measured at 193 and 248 nm dissociation. This energy disposal should be a general behavior for the dissociation from the A band.

The measured branching ratio is 0.18. Recently, Huber and coworkers obtained two NO fragments with different translational energies from the photofragment translational spectra with the ratio of 0.2.<sup>9</sup> According to the theoretical MO calculations, the A band is assigned as the transition  $S_5 \leftarrow S_0$ . The correlation diagram in Appendix predicts that the  $S_5$  state correlates to NO ( ${}^2\Pi_{3/2}$ ) + Cl\*, assuming the  $C_s$  symmetry during the dissociation. This implies that the Cl\* atoms should be exclusively formed from the  $S_5$  state if the dissociation proceeds adiabatically. However, we observed both Cl and Cl\* in the photodissociation of ClNO at 236 nm. One possibility is the fact that if the dissociation is solely from the  $S_5$  state, non-adiabatic transition to other electronic state should occur, which leads to the formation of Cl. It was shown that the non adiabatic couplings during the bond-breaking determine the branching ratio of Cl and Cl\* in the case of photodissociation of HCl.<sup>11</sup>

The branching ratios obtained experimentally fall usually between the values expected from the adiabatic and diabatic limits. The degree of adiabaticity is expressed by the following equation<sup>13</sup>

$$\xi = \left( \frac{R}{v} \right) / \left( \frac{\hbar}{\Delta E} \right)$$

where  $R$  is the length of the interaction region,  $v$  is the relative speed of the separating atoms, and  $\Delta E$  is the energy separation of the interacting states. For a fast dissociation process, the adiabaticity parameter  $\xi$  is small, while the value of  $\xi$  is large for the slow process. The spin-orbit energy separations of each  $j$  states of the atoms are used for the value of  $\Delta E$ , and hence  $\hbar/\Delta E$  is considered as a time for precession of the electrons in the molecule. If the dissociation is slow, the products should be exclusively formed according to the correlation diagram (adiabatic limit), while the products are formed statistically according to the degeneracies of the fine structure states if the dissociation is fast (diabatic limit).

The anisotropy parameter  $\beta$  reveals the angular distribution of the products. When the  $\epsilon$  vector of the dissociating light is perpendicular to the transition dipole moment of the parent molecule,  $\beta$  has the value of  $-1$  and when those directions are parallel,  $\beta$  has the value of 2. It is noticeable that the observed  $\beta$  value of 0.45 for the A band dissociation of ClNO is much smaller than perpendicular or parallel limiting values. The theoretical calculation indicates that in the  $S_5$  state the angle between the transition moment and the N-Cl bond is  $8.9^\circ$ .<sup>3</sup> This implies that the  $\beta$  value from the  $S_5$  dissociation should be near 2 if the ClNO dissociation in the A band is faster than the rotational period of the parent molecule. The low  $\beta$  value obtained for the Cl fragment in this experiment suggests a long lifetime compared to the molecular rotational period as predicted by Bell *et al.*, in the B and C band dissociation.<sup>7</sup> This slow dissociation may result in the high adiabaticity parameter  $\xi$  and hence the dissociation is expected to proceed adiabatically. In addition, the largely different  $\beta$  value of 0.95 for Cl\* formation observed by Haas *et al.*, further suggests that the electronic state which correlates to Cl\* is different from that of Cl.<sup>9</sup> They assumed the two pathways for the dissociation leading to form Cl and Cl\*. Our Doppler profile can be well reproduced from their translational energy distribution and  $\beta$  of

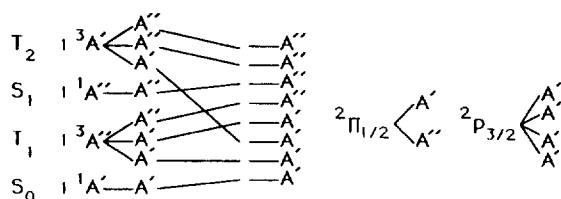
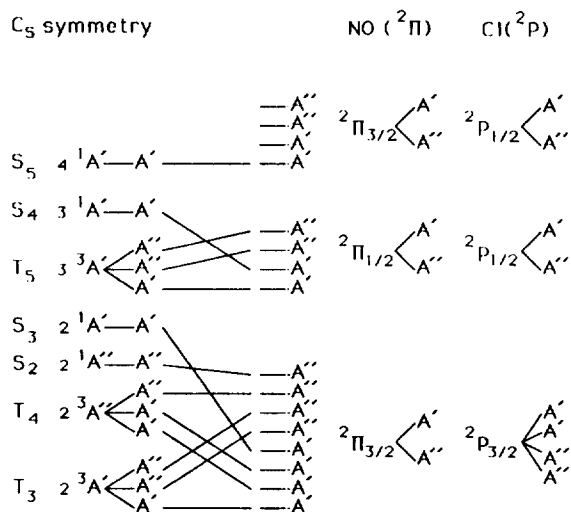
0.45 for Cl. Therefore, we can safely say that the two pathways they observed correspond to the formation of Cl and Cl\*, respectively. As Bai *et al.*, suggested that the broad A band should be composed of a number of excited states other than S<sub>5</sub>,<sup>3</sup> the formation of Cl and Cl\* can thus be explained as more than two electronic states are populated in the excitation at 236 nm and some of them dissociate adiabatically to Cl and NO and others to Cl\*. The excitation of CINO at 236 nm, therefore results in multiple excited states which lead to different dissociation channels.

**Acknowledgement.** This work was supported by the Basic Science Research Institute Program, Ministry of Education of Korea (BSRI 91-301) and partially supported by the Ministry of Education of Japan.

### Appendix

The correlation diagram of CINO to Cl+NO. Electronic states of CINO with C<sub>s</sub> symmetry are from ref. 3 and this C<sub>s</sub> symmetry is assumed to be preserved during the dissociation. This correlation diagram is the revised diagram of Hubers'.<sup>5</sup>

CINO Correlation Diagram



### References

1. "Molecular Photodissociation Dynamics," Ed. by M. N. R. Ashfold and J. E. Baggott, Royal Society of Chemistry, London (1987).
2. G. E. Busch and K. R. Wilson, *J. Chem. Phys.*, **56**, 3655 (1972).
3. Y. Y. Bai, A. Ogai, C. X. W. Quian, G. A. Segal, and H. Reisler, *J. Chem. Phys.*, **90**, 3903 (1988).
4. D. Solgadi, F. Lahmani, C. Lardeux, and J. P. Flament, *Chem. Phys.*, **79**, 225 (1983).
5. A. E. Bruno, U. Bruehlmann, and J. R. Huber, *Chem. Phys.*, **120**, 155 (1988).
6. A. Ticktin, A. E. Bruno, U. Bruehlmann, and J. R. Huber, *Chem. Phys.* **125**, 403 (1988).
7. A. J. Bell, P. R. Pardon, and J. G. Frey, *Mol. Phys.*, **67**, 465 (1989).
8. M. D. Moser, E. Weitz, and G. C. Schatz, *J. Chem. Phys.*, **78**, 757 (1982).
9. B. M. Haas, P. Felder, and J. R. Huber, *Chem. Phys. Lett.*, **180**, 293 (1991).
10. Y. Matsumi, M. Kawasaki, T. Sato, T. Kinugawa, and T. Arikawa, *Chem. Phys. Lett.*, **155**, 486 (1989).
11. Y. Matsumi, P. K. Das, and M. Kawasaki, *J. Chem. Phys.*, **92**, 1696 (1990).
12. (a) R. N. Zare and D. R. Herschbach, *Proc. IEEE*, **51**, 173 (1963); (b) R. N. Dixon, *J. Chem. Phys.*, **85**, 1866 (1986).
13. "Molecular Reaction Dynamics and Chemical Reactivity," R. D. Levin and R. B. Bernstein, Oxford, New York (1987) p. 315.